

Selective etching of TiN over TaN and vice versa in chlorine-containing plasmas

Hyungjoo Shin,^{a)} Weiye Zhu, Lei Liu, Shyam Sridhar, Vincent M. Donnelly,^{b)} and Demetre J. Economou^{c)}

Plasma Processing Laboratory, Department of Chemical and Biomolecular Engineering, University of Houston, Houston, Texas 77204-4004

Chet Lenox and Tom Lii

Texas Instruments Inc., Dallas, Texas 75243

(Received 21 November 2012; accepted 1 April 2013; published 18 April 2013)

Selectivity of etching between physical vapor-deposited TiN and TaN was studied in chlorine-containing plasmas, under isotropic etching conditions. Etching rates for blanket films were measured *in-situ* using optical emission of the N_2 ($C^3\Pi_u \rightarrow B^3\Pi_g$) bandhead at 337 nm to determine the etching time, and transmission electron microscopy to determine the starting film thickness. The etching selectivity in Cl_2/He or HCl/He plasmas was poor ($<2:1$). There was a window of very high selectivity of etching TiN over TaN by adding small amounts ($<1\%$) of O_2 in the Cl_2/He plasma. Reverse selectivity (10:1 of TaN etching over TiN) was observed when adding small amounts of O_2 to the HCl/He plasma. Results are explained on the basis of the volatility of plausible reaction products. © 2013 American Vacuum Society. [<http://dx.doi.org/10.1116/1.4801883>]

I. INTRODUCTION

As the size of features in integrated circuits continues to shrink, metal gates over high-k dielectrics are becoming increasingly important.¹ Currently, the industry is largely moving toward a replacement gate-last integration approach,² to avoid thermal degradation during high temperature activation of implanted dopants, and allow better tuning of the work-function and threshold voltage. The replacement gate-last integration scheme requires removal of very thin (10–30 Å) titanium nitride (TiN) diffusion blocking layers during the “replacement” process, once the poly-Si layer has been removed. The selective removal of these TiN layers from p-type metal-oxide-semiconductor (pMOS) devices enables the independent “tuning”^{3–5} of the work-function metal near the gate, using aluminum diffusion. Etching must be isotropic since the TiN layer must be removed all along the contour of the gate trench. Tantalum nitride (TaN) has been proposed as a potential etch-stop conducting layer for use with this approach. Therefore, a TiN isotropic etching process that stops on TaN is required.

TiN and TaN are also used as antireflective coatings, diffusion barriers, and adhesive or absorber layers in other steps during integrated circuit fabrication. For example, thin films of TiN are used as a barrier to prevent interdiffusion of silicon and aluminum/copper metallization.^{6–9} TiN has the advantages of high thermodynamic stability, good mechanical properties, and low electrical resistivity.

The etching characteristics of TiN (Refs. 10 and 11) or TaN (Refs. 12–15) as a gate material have been studied, focusing on selectivity over high-k dielectrics (e.g., HfO_2). Hwang *et al.*¹⁶ studied etching of TiN and TaN in Cl_2 or HBr gas, using an inductively coupled plasma. The etching

rate of both materials depended on the square root of ion energy (beyond a threshold energy), indicating ion-assisted etching. Addition of a few % O_2 in the feed gas resulted in slowdown of the etching rate of both TiN and TaN. Beyond ~5% oxygen addition, etching was quenched. End-point monitoring of TaN etching in Cl_2 , using the nitrogen 357.7 nm line, showed an induction (breakthrough) period of ~10 min, before etching commenced. Shin *et al.*¹⁷ showed that when the surface of TaN was oxidized, the film could not be etched in $Cl_2/Ar/O_2$ or $HBr/Ar/O_2$ plasmas. However, etching occurred in $BCl_3/Ar/O_2$ plasmas, apparently due to the efficient removal of the oxide layer by BCl_x species. Min *et al.*¹⁸ investigated etching of TiN in an Ar/Cl_2 ICP. The etching rate increased with chlorine content in the feed gas and approached saturation beyond 60% Cl_2 . They measured an etching rate of up to ~5300 Å/min in a plasma with 700 W power, –300 V DC bias, and 5 mTorr pressure. The etching rate increased rather weakly with increasing power (500–900 W range), DC bias voltage (–200 to –400 V), and gas pressure (1–10 mTorr).

Park *et al.*¹⁹ reported etching of TiN in 15 mTorr BCl_3/Cl_2 inductively coupled plasmas at a power of 700 W and a DC bias of –100 V. A maximum etching rate (343 nm/min) was obtained at 25% $BCl_3/75\%$ Cl_2 . Oxygen addition to a 5 sccm $BCl_3/15$ sccm Cl_2 plasma resulted in monotonically diminishing TiN etching rate down to 4 nm/min at 10 sccm O_2 . Comparable additions of argon to the BCl_3/Cl_2 plasma showed minor effects on the etching rate. The authors hypothesized that oxygen addition forms TiO_2 on the surface, which is more difficult to etch compared to TiN. Kim *et al.*²⁰ studied etching of TiN and its selectivity over SiO_2 and HfO_2 films in an ICP with 400–600 W power, –50 to –200 V DC bias, 15 mTorr pressure, 4 sccm BCl_3 , 14 sccm Ar, and variable amounts (0–6 sccm) of Cl_2 . The etching rate increased with chlorine flow rate reaching ~340 nm/min. Etching selectivity over the two oxides also increased with

^{a)}Present address: Lam Research, Fremont, CA.

^{b)}Electronic mail: vmdonnelly@uh.edu

^{c)}Electronic mail: economou@uh.edu

added Cl_2 but the selectivity was always less than 3. Higher (more negative) DC bias enhanced the etching rate of TiN but reduced selectivity. Chiu *et al.*²¹ investigated etching of TiN and TiN/SiO₂ selectivity in Cl_2 helicon plasmas. The substrate electrode was independently powered by a 13.56 MHz power supply. The etching rate of TiN increased with chlorine flow rate, and saturated at higher flows (>70 sccm). As the bias power was increased from 20 W to 70 W, the etching rate of TiN increased to nearly 600 nm/min., but the selectivity toward SiO₂ dropped from ~ 500 to ~ 2 . Vitale *et al.*²² reported etching of TiN by HBr/He/O₂ in an ICP, for fabricating metal gates for silicon-on-insulator transistors. Under the conditions studied, etching was limited by the ion flux. In the absence of substrate bias, TiN was chemically etched by Br atoms. Oxygen addition to HBr strongly inhibited etching of TiN, apparently through competitive adsorption of O atoms on the surface of the film. Process optimization led to a selectivity of TiN/SiO₂ of nearly 1000.

In the above work, etching of TiN and/or TaN was studied focusing on the potential use of these materials as metal gates, replacing polysilicon. Thus, selectivity was sought over gate oxide materials (HfO₂, SiO₂ etc.) The present work emphasizes use of TiN over TaN as very thin films lining the gate structure in gate-last integration schemes. As such, selectivity of TiN over TaN is required. A high etching rate is not important since the films are very thin (10–30 Å). Studies of selectivity of TiN over TaN (or vice versa) apparently have not been reported previously.

II. EXPERIMENT

Blanket TiN and TaN films with average thickness of 375 ± 20 Å and 635 ± 30 Å, respectively, were deposited on Si wafers by physical vapor deposition. Film thicknesses were measured by ellipsometry and confirmed by transmission electron microscopy (TEM). Small pieces ($\sim 1 \text{ cm} \times 1.5 \text{ cm}$) cut from the wafer were used for etching. Samples were cleaned using isopropyl alcohol and blown dry with nitrogen just before inserting into the reactor.

A. Plasma etching reactor

The plasma etching reactor, shown schematically in Fig. 1, has been described in detail before.²³ A 13.56 MHz inductively coupled plasma (ICP) was generated in a 9.5 cm diam. alumina tube that was surrounded by a Faraday shield and a helical coil. Gas was injected from an opening at the center of the top flange and was pumped by 300 l/s turbomolecular pump (EBARA ET300WS). While the pumping speed could be varied using a throttle valve, in most experiments, the valve was fully open, to achieve the maximum possible feed gas flow and minimize the partial pressure of any contaminants leaking from the atmosphere or outgassing from the chamber walls. The outgassing/leak rate, as measured by the pressure rise method, corresponded to a flow rate of 1.6×10^{-4} sccm (standard cm³/min). The chamber base pressure was 8×10^{-8} Torr. Samples mounted on a 1 in. diam. stainless steel sample puck using double-sided carbon tape were introduced into the reactor through a load-lock

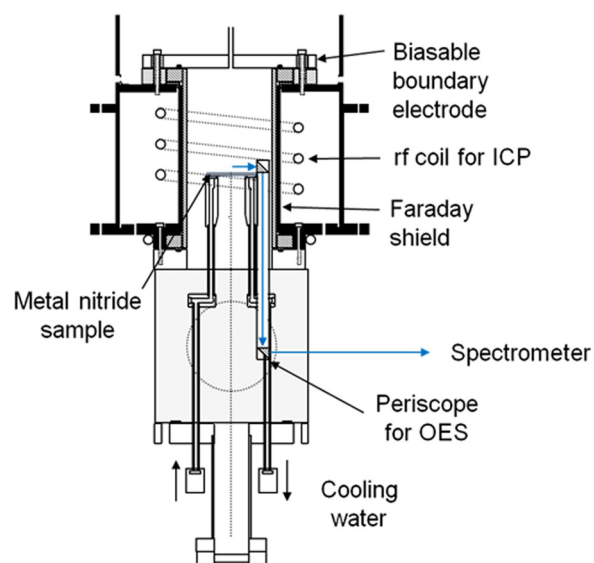


Fig. 1. (Color online) Schematic of the Faraday-shielded, inductively coupled plasma reactor. A periscope was used to collect optical emission from the region near the sample surface. Samples could be transferred under vacuum to an x-ray photoelectron spectrometer (XPS). More details of the experimental apparatus can be found in Ref. 23.

chamber. Processed samples could be transferred to an adjacent x-ray photoelectron spectroscopy (XPS) chamber (Surface Science M-probe, Service Physics Inc.) without exposure to atmosphere. A closed loop chiller was used to control the substrate temperature at 60 °C.

A periscope with two right angle quartz prisms collected plasma emission from a small distance above the sample. The light passed through a quartz window and then was focused with a fused silica lens onto the entrance slit of a monochromator (Heath Co.), equipped with a GaAs photomultiplier tube. The spectral resolution was 2.2 Å with a slit width of 100 μm. Optical emission spectroscopy in this system provided end-point curves that were used to obtain the etching rate of the TiN and TaN films *in situ*.

The baseline etching conditions were as follows: 420 W plasma power, no bias power, and 35 mTorr pressure. A total flow rate of 300 sccm was used for most experiments. The gas composition was varied between 2% and 25% Cl_2 in Ar, or 3.3% and 50% HCl in He. For some experiments, a trace amount of oxygen was added to the feed gas. A mass flow controller was used for O₂ flows >0.5 sccm. At lower flows, a leak valve was used, with the following calibration procedure. Pressure was measured with an ionization gauge when flowing only O₂ into the chamber with the throttle valve at a known position. The throttle valve was then quickly closed and a pressure rise, dP/dt , was recorded as the gas filled the known chamber volume (determined from a prior dP/dt measurement with a known flow of Ar). In these measurements, the base pressure was subtracted from the O₂ pressure measurement and dP/dt resulting from outgassing and/or leaks, recorded with no gas flowing, was subtracted from dP/dt measured with O₂ flow. Various flows were established to generate a calibration curve of O₂ flow rate versus pressure. Any flow of O₂ could then be obtained by establishing an O₂

flow with the throttle valve in the original position, recording the pressure with the ionization gauge, and interpolating the calibration plot of O_2 flow rate versus pressure.

When using a small fraction of Cl_2 in He, it was difficult to ignite and/or sustain the plasma, apparently because of the large ionization potential of He, and the presence of a Faraday shield, which prevented capacitive coupling. In such cases, Ar instead of He was used as the carrier gas. The lack of capacitive coupling resulted in very low plasma potential, which allowed the energy of ions impacting the unpowered sample stage to be held below ~ 15 eV.²³ Under these conditions, ion-assisted etching of the sample should be negligible and isotropic etching should prevail.

B. End-point detection

Figure 2(a) shows optical emission intensity as a function of time for the N_2 ($C^3\Pi_u \rightarrow B^3\Pi_g$) bandhead at 337 nm, and the Si 288 nm line during TiN etching. N_2 was a product of TiN etching, while Si originated from the underlying substrate. Once the plasma was turned on, N_2 emission appeared, reached a maximum, and then decayed to the background level of ~ 0.13 arbitrary units (a.u.), signifying

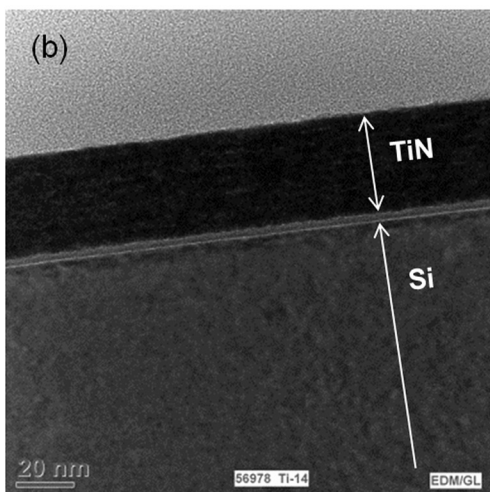
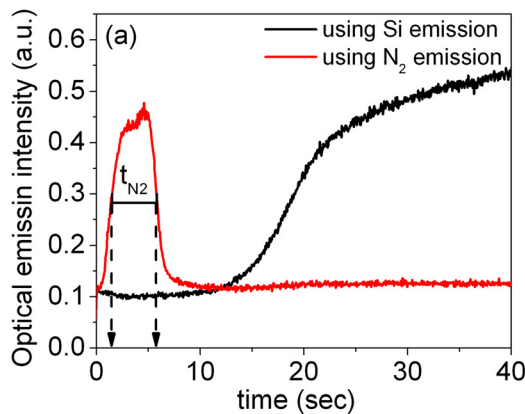


FIG. 2. (Color online) (a) Optical emission intensity of N_2 ($C^3\Pi_u, \nu' = 0 \rightarrow B^3\Pi_g, \nu'' = 0$) at 337 nm and Si at 288 nm as a function of time during etching of a 375 ± 20 Å nm thick TiN film on a Si substrate in a 30% HCl /70% He plasma at 35 mTorr and 420 W. (b) Cross sectional TEM of a TiN/Si sample. The TiN film etching time was taken as t_{N_2} .

that the nitride film was completely removed (end-point). In contrast, the Si emission remained at the background level until after the end-point of TiN etching. The delay in Si signal rise with respect to the cessation of N_2 emission was due to a 1–2 nm-thick interfacial layer between TiN and Si, confirmed by TEM [Fig. 2(b)]. Apparently, this film did not contain much nitrogen (if any) and/or etched very slowly. Once this film was etched through, Si emission started to increase steadily. The etching rate of TiN was calculated based on the initial TiN film thickness, and the average time it took to completely etch the film, which was taken as the full width at half maximum (FWHM) of the N_2 emission signal versus time [t_{N_2} in Fig. 2(a)].

TaN etching showed different behavior [Fig. 3(a)] compared to TiN. N_2 emission began to rise above the background level of ~ 0.2 a.u. a considerable time after the plasma was turned on, and returned to the background at a later time. This induction period before TaN etching commenced [time t_0 in Fig. 3(a)] was due to a very thin native oxide on the surface,^{16,17} not visible by low resolution TEM [Fig. 3(b)], but confirmed by XPS. Unlike TiN, Si emission rose sharply as the last of the TaN film was etched away and

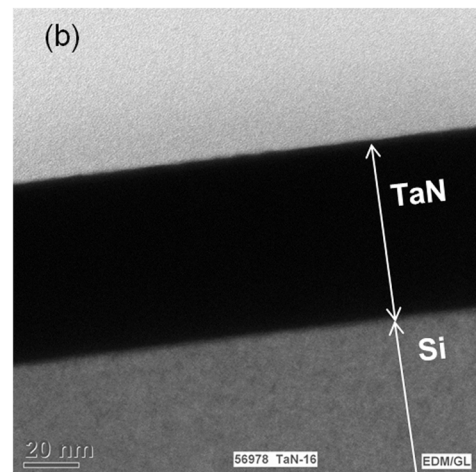
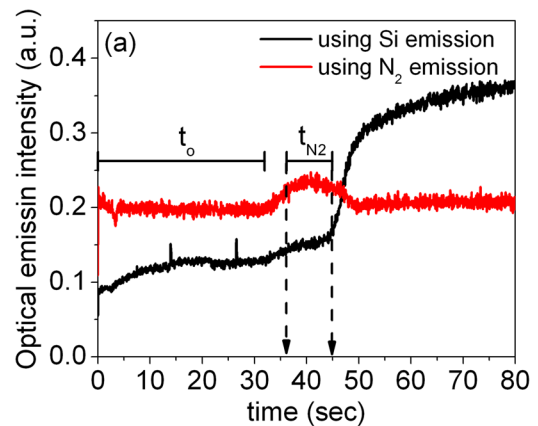


FIG. 3. (Color online) (a) Optical emission intensity of N_2 ($C^3\Pi_u, \nu' = 0 \rightarrow B^3\Pi_g, \nu'' = 0$) at 337 nm and Si at 288 nm as a function of time during etching of a 635 ± 30 Å nm thick TaN film on a Si substrate in a 30% HCl /70% He plasma at 35 mTorr and 420 W. (b) Cross sectional TEM of a TaN/Si sample. The TaN film etching time was taken as t_{N_2} . The induction period is shown as t_0 .

the N₂ signal began to decay, indicating fast etching of a very thin interfacial layer. The initial TaN film thickness was divided by the etching time t_{N_2} (again, FWHM of N₂ signal), to obtain the etching rate. N₂ emission (and not Si emission) was used for end-point detection to avoid the complexity of correcting for the long induction period before etching of TaN begins.

III. RESULTS AND DISCUSSION

A. Cl₂/Ar plasmas

Figures 4(a) and 4(b) show the N₂ optical emission traces during etching of TiN and TaN, respectively, in 35mTorr, 420 W Cl₂/Ar plasmas with different amounts of Cl₂. The curves have been normalized, as the optical emission intensity depends on plasma parameters (electron density and temperature) that change as the Cl₂ content varies. The induction period (t_0), before etching of TaN commences, increases as the %Cl₂ decreases. An appreciable induction period is also observed in TiN etching when using small amounts of Cl₂ (<2%). Figure 5 is a summary of the etching rates as a function of Cl₂ addition to Ar. It was confirmed

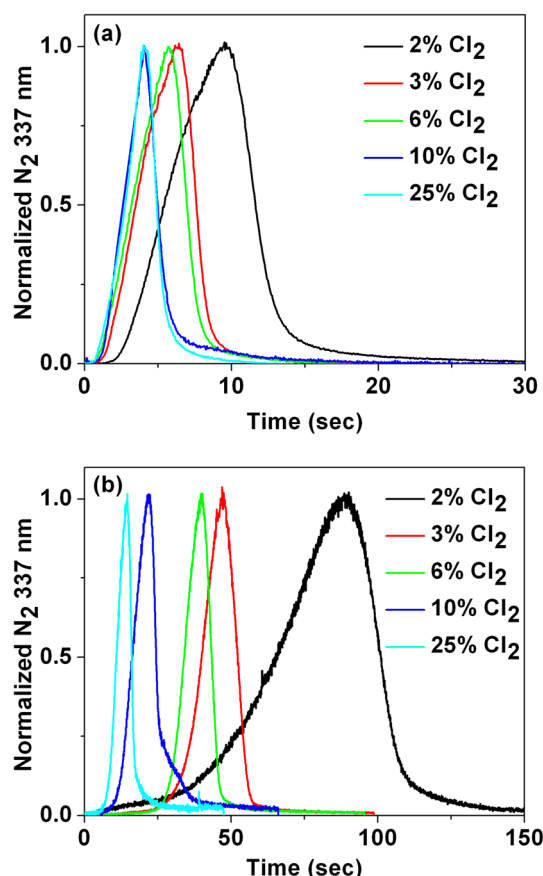


FIG. 4. (Color online) Normalized optical emission intensities of N₂ ($C^3\Pi_u, \nu' = 0 \rightarrow B^3\Pi_g, \nu'' = 0$) at 337 nm as a function of time during etching of TiN and TaN films on Si substrates in Cl₂/Ar plasmas for different %Cl₂. Pressure = 35 mTorr; power 420 W. (a) TiN film. Signal intensities were normalized by multiplying by 0.3, 0.27, 0.35, 0.64, and 0.45 for 2, 3, 6, 10, and 25% Cl₂, respectively. (b) TaN film. Signal intensities were normalized by multiplying by 1.5, 0.6, 0.56, 1.25, and 1.72 for 2, 3, 6, 10, and 25% Cl₂, respectively.

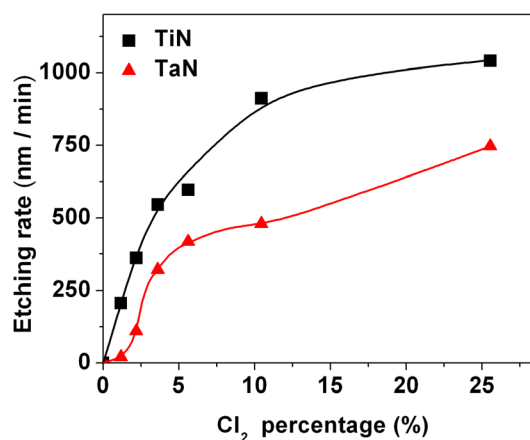


FIG. 5. (Color online) Etching rate of TiN and TaN in Cl₂/He plasma at 35 mTorr and 420 W as a function of %Cl₂. The lines are simply to guide the eye.

that the etching rate of either film was immeasurably slow in the absence of Cl₂. The etching rate increases rapidly at low %Cl₂ and starts to saturate at large %Cl₂.

TaN etches slower than TiN, and this correlates with the lower vapor pressure of TaCl₅ (estimated as $\sim 10^{-2}$ Torr, extrapolated from higher temperature to 333 K, the substrate temperature²⁴), relative to TiCl₄ [~ 60 Torr at 333 K (Ref. 25)]. A slower etching of TaN compared to TiN in chlorine-containing plasmas has been reported before.^{16,26} Based on the results of Fig. 5, the selectivity of etching TiN over TaN is poor (less than 2:1). Selectivity can be greatly improved by introducing small amounts of oxygen in the plasma, as shown next.

B. Cl₂/He/O₂ plasmas

A 25% Cl₂/75% He plasma at 35mTorr was chosen to study the effect of O₂ addition on the etching rates of TiN and TaN. Once the oxygen flow was stabilized, 7.5 sccm of Cl₂ and 51 sccm of He were added to the feed gas. For O₂ additions greater than $\sim 0.5\%$, no N₂ emission, and hence no TaN etching, was detected over a 30-min plasma exposure. Postetching XPS spectra showed Ta, O, and N on the surface, but no Si, suggesting that the remaining TaN layer was >10 nm thick (enough to attenuate to undetectable levels any photoelectrons originating from the Si underneath). Apparently, the native oxide of TaN blocks etching under these conditions.

To separate the influence of the native oxide on TaN from the true dependence of the etching rate of TaN on O₂ concentration, the native oxide was first removed in the Cl₂/He plasma with no added O₂. The end of the induction period corresponded to the moment when the N₂ signal was first detected above the baseline. At that point, the plasma was extinguished, the desired flow of O₂ was added to the Cl₂/He gas flow, and the plasma was reignited while monitoring N₂ emission to measure t_{N_2} . For TiN, the native oxide breakthrough occurs rapidly (few seconds); hence, little error is made in ignoring it in measuring etching times and rates. Following the above procedure, TiN and TaN etching rates

were measured as a function of O₂ addition (Fig. 6). When the O₂ percentage was below 0.3, there was essentially no influence on the etching rates. Above 0.3%, O₂ addition depressed the etching rate of both TiN and TaN. However, the etching rate of TiN slowed gradually, up to an O₂ percentage of 0.9, while the etching rate of TaN dropped precipitously for O₂ percentages higher than 0.3. There is a window of oxygen percentage (0.3%–0.7%) that provides very high selectivity of etching TiN over TaN. It should be noted that, even in the case of TiN, end-point detection became increasingly more difficult as the etching rate decreased, for relatively high oxygen additions. In such cases, XPS was used to verify that no TiN remained on the surface at end-point.

Under low ion bombardment energy (less than 15 eV), the rate limiting step in etching is likely to be either formation of the etching products or vaporization of these products. TiOCl₂ and TaOCl₃ are the most stable products formed in the reaction of TiCl₄ and TaCl₅ with O₂.^{27,28} Apparently, the vapor pressure is unknown for TiOCl₂, but this species has been identified by mass spectrometry in the gas phase, surviving transport through water-cooled tubing.²⁷ It is therefore reasonable to assume that TiOCl₂ has an appreciable vapor pressure. Conversely, extrapolating from high temperature data,²⁹ we estimate that the vapor pressure of TaOCl₃ at 333 K is $\sim 10^{-12}$ Torr. Therefore, once enough oxygen is added to the plasma for TaOCl₃ to form, further etching is blocked. For TiN, at high enough oxygen addition, a layer that is more heavily oxidized than TiOCl₂ may form that blocks etching.

C. HCl/He and HCl/He/O₂ plasmas

Etching of TiN and TaN films was also investigated in 35 mTorr, 420 W HCl/He plasmas. Figure 7 shows the etching rate versus %HCl. Similar to Cl₂/He plasmas, etching rates increase rapidly at low %HCl and start to saturate with higher %HCl. The TaN etching rate is slower than that of TiN with less than 30% HCl, and becomes comparable at 50% HCl. Comparing Figs. 7 and 5 at 25% HCl and Cl₂, respectively, the etching rate of TiN and TaN in the HCl/He

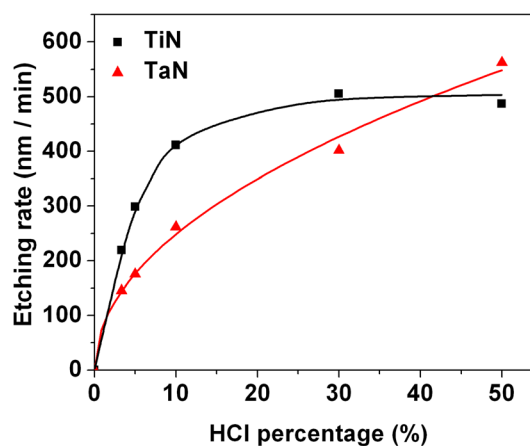


Fig. 7. (Color online) Etching rates of TiN and TaN in HCl/He plasma at 35 mTorr and 420 W as a function of %HCl. The lines are simply to guide the eye.

plasma is approximately 50% of that in the Cl₂/He plasma. This could be due to lower Cl atom number density in the HCl/He plasma.

Etching of TiN and TaN films was also investigated in 30% HCl/70% He plasmas with small amounts of O₂ addition. The HCl and He flow rates were 90 and 210 sccm, respectively, and the total pressure was 35 mTorr (the same as in the Cl₂/He plasma). The reactor base pressure (8.0×10^{-8} Torr), was much lower than the smallest controlled partial pressure of oxygen examined. Similar to etching in Cl₂/He plasmas, O₂ was added to the plasma feed gas after an induction period t_0 ended for removing the native oxide layer from TaN. Figure 8 shows etching rates as a function of added O₂. The etching rate of TiN starts to gradually decrease with small O₂ additions and stops at about 0.27% O₂. For TaN, however, etching rates were not affected by O₂ addition until the O₂ percentage reached $\sim 0.2\%$, above which the etching rate dropped precipitously. Thus, it is possible to achieve high selectivity ($\sim 10:1$) for etching TaN over TiN in HCl/O₂/He plasmas, the reverse of that obtained in Cl₂/O₂/He plasmas.

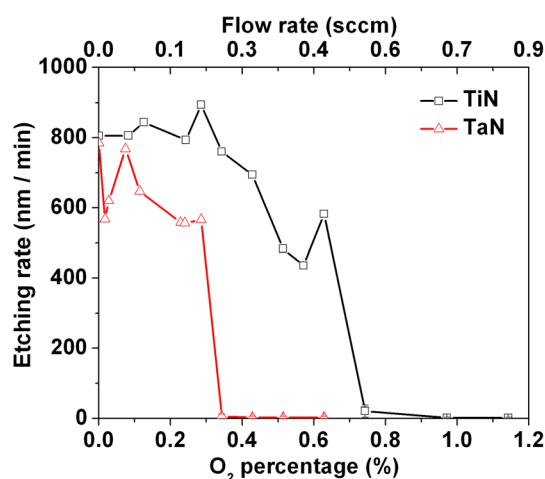


Fig. 6. (Color online) Etching rate of TiN and TaN in 25%Cl₂/O₂/He plasma at 35 mTorr and 420 W as a function of added %O₂. The lines are simply to guide the eye.

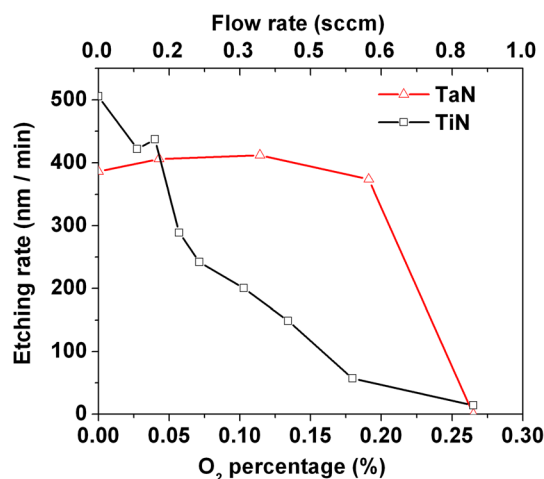


Fig. 8. (Color online) Etching rates of TiN and TaN in 30%HCl/O₂/He plasma at 35 mTorr and 420 W as a function of added %O₂. The lines are simply to guide the eye.

Given the ~30%–50% slower etching in oxygen-free HCl/He plasmas versus Cl₂/He plasmas, it seems that O₂ addition has little effect on the TaN etching rate, but instead causes a large suppression in the TiN etching rate. H atoms could simply block sites for Cl adsorption and slow etching. Alternatively, since H₂O forms in HCl/O₂-containing plasmas and TiOCl₂ is known to form complexes with HCl and H₂O,^{30,31} perhaps desorption of TiOCl₂ is inhibited by formation of complexes such as TiOCl₂·H₂O_x·HCl_y.

In both Cl₂-containing and HCl-containing plasmas, it takes considerably less added O₂ to stop TaN etching when the native oxide is present on the film surface. For example, etching of TaN with native oxide can be turned off with less than 4×10^{-5} Torr of O₂, whereas TaN without native oxide can still be etched through by 7×10^{-5} Torr of O₂ addition in HCl/He plasmas. It is likely that the starting oxide thickness plays a critical role in the etching or further growth of the oxide layer on top of metal nitrides. A similar observation has been made for SiO₂ etching or growth on Si substrate using 10%O₂/90%HBr plasmas.³² Oxide films with initial thickness greater than 15 Å grew and reached a self-limited thickness of 33 Å over long plasma exposure; SiO₂ films with initial thickness less than 15 Å were completely etched away. It is thus likely that the native oxide is too thick to be etched faster than it can grow, when the percent O₂ is greater than 1% in Cl₂/He/O₂ plasmas, and 0.27% in HCl/He/O₂ plasmas.

Finally, it should be noted that this study was performed with blanket films formed by physical vapor deposition. Results could be different for films grown by chemical vapor deposition. Since it takes so little oxygen addition to slow the etching rate of TaN in Cl₂-containing plasmas and TiN in HCl-containing plasmas, the unintentional addition of oxygen from leaks, chamber outgassing and etching or erosion of masks, other substrate materials or reactor parts, could be important. Perhaps other contaminants such as carbon from photoresist etching could also play an important role. Consequently, the amount of O₂ addition needed to achieve high selectivity would need to be adjusted in commercial plasma etching processes, and/or the total gas flow rate would need to be increased.

IV. SUMMARY AND CONCLUSIONS

Selective etching between blanket PVD TiN and TaN was investigated in chlorine-containing inductively coupled plasmas, under isotropic etching conditions (ion energy < 15 eV, i.e., below the threshold for ion-assisted etching). Etching rates were measured *in-situ* using optical emission of the N₂ (C³Π_u → B³Π_g) bandhead at 337 nm to determine the etching time, and transmission electron microscopy to determine the starting film thickness. Etching rates were relatively high (up to 1000 Å/min), despite the absence of ion-assisted etching. In Cl₂/He or HCl/He plasmas, the etching rate of both TiN and TaN at first increased rapidly with increasing %Cl₂ or %HCl, but it appeared to saturate at higher percentage of halogen addition. Generally, TiN etched faster than TaN in these plasmas, but the selectivity was poor (less than 2:1). However, by adding small amounts (<1% by volume) of O₂

to the Cl₂/He plasma, there was a window (0.3–0.7%) of O₂ addition that resulted in very high selectivity of etching TiN over TaN. This may be caused by the difference in volatility of the plausible reaction products: TaOCl₃ is nonvolatile, whereas TiOCl₂ is volatile under the reaction conditions. Furthermore, by adding small amounts (<0.3%) of O₂ in HCl/He plasmas, up to 10:1 selectivity of etching TaN over TiN (reverse selectivity) was observed.

ACKNOWLEDGMENTS

This work was supported by Texas Instruments Inc. The authors thank Dan Corum, Robert Turner, and Fred Clark for performing TEM and SEM measurements.

- ¹B. H. Lee, S. C. Song, R. Choi, and P. Kirsch, *IEEE Trans. Electron Devices* **55**, 8 (2008).
- ²A. Chatterjee *et al.*, Tech. Dig. - Int. Electron Devices Meet. **1998**, 777.
- ³C. Ren *et al.*, *Appl. Phys. Lett.* **87**, 073506 (2005).
- ⁴X. P. Wang *et al.*, *IEEE Trans. Electron Devices* **54**, 2871 (2007).
- ⁵R. Singanamalla, H. Y. Yu, B. Van Daele, S. Kubicek, and K. De Meyer, *IEEE Electron. Dev. Lett.* **28**, 1089 (2007).
- ⁶C. Y. Ting and M. Wittmer, *Thin Solid Films* **96**, 327 (1982).
- ⁷C. Y. Ting, *J. Vac. Sci. Technol.* **21**, 14 (1982).
- ⁸M. Wittmer, *J. Vac. Sci. Technol. A* **3**, 1797 (1985).
- ⁹I. Suni, M. Blomberg, and J. Saarilahti, *J. Vac. Sci. Technol. A* **3**, 2233 (1985).
- ¹⁰J. Tonotani, T. Iwamoto, F. Sato, K. Hattori, S. Ohmi, and H. Iwai, *J. Vac. Sci. Technol. B* **21**, 2163 (2003).
- ¹¹A. L. Gouil, O. Joubert, G. Cunge, T. Chevolleau, L. Vallier, B. Chenevier, and I. Matko, *J. Vac. Sci. Technol. B* **25**, 767 (2007).
- ¹²V. N. Bliznetsov, L. K. Bera, Haw Yun Soo, N. Balasubramanian, R. Kumar, G.-Q. Lo, W. J. Yoo, C. H. Tung, and L. Linn, *IEEE Trans. Semicond. Manuf.* **20**, 143 (2007).
- ¹³V. Bliznetsov, R. Kumar, L. K. Bera, L. W. Yip, A. Du, and T. E. Hui, *Thin Solid Films* **504**, 140 (2006).
- ¹⁴K. Nakamura, T. Kitagawa, K. Osari, K. Takahashi, and K. Ono, *Vacuum* **80**, 761 (2006).
- ¹⁵M. H. Shin, S. W. Na, N.-E. Lee, and J. H. Ahn, *Thin Solid Films* **506–507**, 230 (2006).
- ¹⁶W. S. Hwang, J. Chen, W. J. Yoo, and V. Bliznetsov, *J. Vac. Sci. Technol. A* **23**, 964 (2005).
- ¹⁷M. H. Shin, M. S. Park, N.-E. Lee, J. Kim, C. Y. Kim, and J. Ahn, *J. Vac. Sci. Technol. A* **24**, 1373 (2006).
- ¹⁸S. R. Min, H. N. Cho, Y. L. Li, S. K. Lim, S. P. Choi, C. W. Chung, *J. Ind. Eng. Chem. (Seoul, Repub. Korea)* **14**, 297 (2008).
- ¹⁹J.-S. Park, J.-C. Woo, and C.-I. Kim, *Jpn. J. Appl. Phys.*, **50**, 08KC01 (2011).
- ²⁰D.-P. Kim, X. Yang, J.-C. Woo, D.-S. Um, and C.-I. Kim, *J. Vac. Sci. Technol. A*, **27**, 1320 (2009).
- ²¹H. K. Chiu, T. L. Lin, Y. Hu, K. C. Leou, H. C. Lin, M. S. Tsai, and T. Y. Huang, *J. Vac. Sci. Technol. A*, **19**, 455 (2001).
- ²²S. A. Vitale, J. Kedzierski, and C. L. Keast, *J. Vac. Sci. Technol. B*, **27**, 2472 (2009).
- ²³H. Shin, W. Zhu, L. Xu, V. M. Donnelly, and D. J. Economou, *Plasma Sources Sci. Technol.* **20**, 055001 (2011).
- ²⁴J. M. Brink and F. D. Stevenson, *J. Chem. Eng. Data* **17**, 143 (1972).
- ²⁵M. L. Pearce and N. R. McCabe, *J. Inorg. Nucl. Chem.* **27**, 1876 (1965).
- ²⁶R. Ramos, G. Cunge, and O. Joubert, *J. Vac. Sci. Technol. B* **26**, 181 (2008).
- ²⁷B. Karlemo, P. Koukkari and J. Paloniemi, *Plasma Chem. Plasma Processing* **16**, 59 (1996).
- ²⁸J. Aarik, K. Kukli, A. Aidla, and L. Pung, *Appl. Surf. Sci.* **103**, 331 (1996).
- ²⁹A. Vértes, S. Nagy, Z. Klencsár, R. G. Lovas, and F. Rösch, *Handbook of Nuclear Chemistry*, 2nd ed. (Springer, New York, 2011), pp. 934.
- ³⁰M. Madekufamba, L. N. Trevani, and P. R. Tremaine, *J. Chem. Thermodynam.* **38**, 1563 (2006).
- ³¹J.-K. Park and H.-K. Kim, *Bull. Korean Chem. Soc.* **23**, 745 (2002).
- ³²V. M. Donnelly, F. P. Klemens, T. W. Sorsch, G. L. Timp, and F. H. Baumann, *Appl. Phys. Lett.* **74**, 1260 (1999).